

## Supporting Information

### The right nanoparticle size for the right job – designing novel ZnO electrode architectures for efficient dye-sensitized solar cells†

Markus W. Pfau<sup>a,c,d,‡</sup>, Andreas Kunzmann<sup>a,‡</sup>, Doris Segets<sup>b</sup>, Wolfgang Peukert<sup>b</sup>, Gordon G. Wallace<sup>c</sup>, David L. Officer<sup>c</sup>, Tim Clark<sup>d</sup>, Rubén D. Costa<sup>a,\*</sup> and Dirk M. Guldi<sup>a,\*</sup>

#### Experimental

##### Materials

The 20 nm ZnO nanoparticles (Zinc(II) oxide powder, 99.5%, monodisperse, lolitec), ethanol methylethylcellulose (5-15 mPas#46070 and 30-50 mPas#46080, Aldrich) and triacetine (1,2,3-triacetoxyp propane, Sigma-Aldrich, Germany) were bought and used without further purification. The ruthenium dye (N719) was obtained from Solaronix (Aubonne, Switzerland). For the synthesis of the 10 nm ZnO particles featured in the transparent electrodes we used zincacetate (Sigma-Aldrich, ACS reagent, ≥99,0%), methanol (Chromanorm, ≥99,80%) and tetramethylammonium hydroxide (Sigma-Aldrich, 25wt. % in methanol). For 2 nm ZnO particles used for the buffer layer, we used zinc acetate dihydrate (ACS grade, 98.0-101.0 %, VWR Germany), lithium hydroxide (98%, VWR Germany), and ethanol (99.98%, VWR Germany).

##### Nanoparticle preparation

As mentioned, 20 nm ZnO nanoparticles were used as received from the manufacturer. The 10 nm ZnO nanoparticles were synthesized in accordance with our previously published method adding TMAOH as hydroxide source to a methanolic zinc acetate solution at 75 °C.<sup>1</sup> Particles were isolated after several days of reflux by precipitation with heptane followed by washing with ethanol. The 2 nm ZnO nanoparticles were prepared according to our previously published procedure using ethanol as solvent and LiOH as hydroxide source.<sup>2,3</sup> In detail, a zinc acetate precursor solution was obtained by refluxing 0.1 M zinc acetate for 3 h in ethanol at 80 °C in a rotary evaporator.<sup>4</sup> A 0.1 M lithium hydroxide solution was prepared simultaneously by gentle heating (50 °C) and sonication. After cooling to room temperature, the two solutions were mixed and subsequently particle formation set in. To obtain small particle sizes, the nanoparticles were immediately flocculated by adding heptane.<sup>5</sup> The flocculates were centrifuged, carefully rinsed with ethanol to remove excess heptane, and dried at room temperature under vacuum. Particle size distributions (PSDs) of the small ZnO nanoparticles were derived from UV/Vis absorbance spectra as reported in previous studies – see following section for more details.<sup>5</sup>

##### Characterization of ZnO nanoparticles

The characterization of the small nanoparticles was performed by UV/Vis absorbance spectroscopy (Cary 100 Scan, Varian Deutschland GmbH, Germany). Absorbance measurements were converted to particle size distributions (PSDs) according to Segets *et al.*,<sup>2,3</sup> assuming an additive superposition of differently sized particle fractions.<sup>6-8</sup> For the bulk absorption, the data of Bergström<sup>9</sup> was used and, for the correlation between band gap shift and particle size, we used the well-established tight binding model (TBM) of Viswanatha *et al.*<sup>10</sup> Indeed, the methods mentioned above have been carefully cross-validated against TEM, AUC and SAXS measurements.<sup>11,12</sup> The XRD measurements were carried out using a FBruker D8 Advance in Bragg Brentano, featuring a Vantec1 Detector.

##### Paste preparation

The ZnO nanoparticles for the light scattering layer were mixed by weighing the 10 and 20 nm particles in either 1:5, 1:10 or 1:20 mass ratios. The ZnO nanoparticle pastes were prepared by mixing 20 % (w/w) of the desired nanoparticles or nanoparticle mixtures with 7 % (w/w) methylethylcellulose (5-15 mPas and 30-50 mPas, in a 1:1 ratio) and 3 % (w/w) triacetin in EtOH (70 % w/w) and slowly stirred for 3 days until a homogenous paste was obtained. The nanoparticle percentage was confirmed with TGA measurements. The pastes used for decreasing the thickness of the buffer layers were obtained *via* dilution with EtOH – *i.e.*, 300 µL EtOH for 100 mg ZnO nanoparticles and a subsequent dilution of 2, 3, 4, and 5 times, yielding a 100 nm thick layer for a dilution factor of 5.

##### ZnO film characterization

The surface morphology was investigated *via* scanning electron microscopy (SEM) using a Zeiss Gemini 55 Ultra under vacuum (10<sup>-9</sup> mbar). For the cross-section SEM picture, the corresponding electrode was broken through the center and then investigated. Absorption, transmittance, and diffuse reflectance assays were performed with a Varian Cary 5000 spectrophotometer equipped with an integrating sphere. The data was acquired with the Cary WinUV software. The diffuse reflectance was measured using a Spectralon waiver as a reference. Bulk resistance measurements of the different electrodes were obtained by using the four-point probe technique. These measurements were performed with a homemade instrument that consists of a linear pin configuration with a pin gap of 1 mm that are directly connected to a Keithley 2400 SourceMeter. The layer thickness was measured using the DektakXT profilometer from Bruker and an averaging of up to five measurements was always performed. The roughness average was calculated by accumulating profilometry scans and using the analytical Gaussian method implemented in the software.

### Device assembly

FTO TEC 15 substrates (Xop Glass Company) were cleaned with an alkaline surfactant solution (Deconex FPD 120, 1 % vol. solution in 150 ml deionized water) in an ultrasonication bath for 15 min. Afterwards, the substrates were rinsed with water and sonicated in deionized water for 15 min. Finally, the substrates were sonicated in isopropyl alcohol for a further 15 min and, subsequently, dried in a nitrogen flow. To completely clean the surface from any organic contaminants, the substrates were placed in an UV-O<sub>3</sub> cleaner (Jelight Model 42-220) for 18 min. The prepared ZnO pastes were doctor-bladed using a circular template with a diameter of 5 mm and a thickness of 50 µm onto a FTO slide. For multilayer fabrication, the underlying layers were first dried at 85 °C for 8 minutes before the next layer would be applied. The latter were subsequently sintered from room temperature to 500 °C with sequential sintering steps up to 150 °C with a ramp of 10 °C/min for 10 min, up to 325 °C with a ramp of 15 °C/min for 5 min, up to 375 °C with a ramp of 5 °C/min for 5 min, up to 450 °C with a ramp of 7 °C/min for 30 min, and finally up to 500 °C with a ramp of 5 °C/min for 15 min. After cooling to 80 °C, they were immersed into an ethanol:isopropanol solution of N719 ( $2 \times 10^{-4}$  M) for 90 min. Notably, different sintering ramps for photoanode production have been thoroughly investigated with maximum temperatures ranging from 300 to 550°C. During this study, it became evident that the highest efficiencies could be achieved when employing a ramp featuring 500°C as maximal temperature. For counter-electrode fabrication, FTO plates with two holes of 1 mm in diameter at the edge of the active area were used. The FTO slides were cleaned following the aforementioned procedure, after the drilling. Onto the clean FTO substrates an isopropanol solution of 0.5 mmol H<sub>2</sub>PtCl<sub>6</sub> prepared from chloroplatinic acid hydrate ~38 % Pt basis was drop casted forming a thin film of chloroplatinic acid. The FTO plates were dried in air for 5 min and sintered at 400 °C for 20 min. Subsequently, both electrodes were sealed together with a transparent film of Surlyn 25 µm (DuPont Ltd., UK) cut as a rectangular frame around the nanocrystalline film. A solution of 0.6 M 1-butyl-3-methylimidazolium iodide 99 %, 0.03 M iodine, 0.1 M guanidine thiocyanate ≥99.0 %, and 0.5 M 4-tert-butylpyridine 96 % in a mixture of acetonitrile and valeronitrile (85:15) was used as electrolyte. The latter was introduced through the holes in the counter-electrode and immediately sealed. The values presented herein are an average of 5 or more devices usually prepared at different days with different pastes to minimize external influences.

### Device characterization

Electrochemical impedance spectroscopy (EIS) was performed using a potentiostat/galvanostat (PGSTAT30, Autolab) equipped with a frequency response analyzer module (FRA). Measurements were performed at the respective open-circuit voltage of the different devices under dark and illumination (AM 1.5 filter, 100 W/cm<sup>2</sup>) conditions. The AC signal amplitude was set at 10 mV, modulated in a frequency range from 0.1 to 100 KHz. The Nova version 1.10 software was used to obtain the parameters from the equivalent circuit. Photocurrent measurements were carried out under AM 1.5 conditions using a custom-made solar simulator, featuring a 140-160 Watt adjustable Xe lamp source (LOT) combined with an appropriate AM 1.5 filter. Current voltage measurements were recorded by using a potentiostat/galvanostat (PGSTAT30, Autolab) in the range of -0.8 to 0.2 V. Incident photon-to-current efficiency (IPCE) spectra were measured by using Newport apparatus model 70104. For desorption studies, the sensitized photoanodes were immersed into a 1 M NaOH solution for 1 minute. The resulting dye solution was measured in a UV/Vis spectrometer (Shimadzu UV-3102 UV-VIS-NIR Scanning Spectrophotometer) alongside a stock solution with predetermined concentration. After gathering this information the dye-loading could then be calculated.

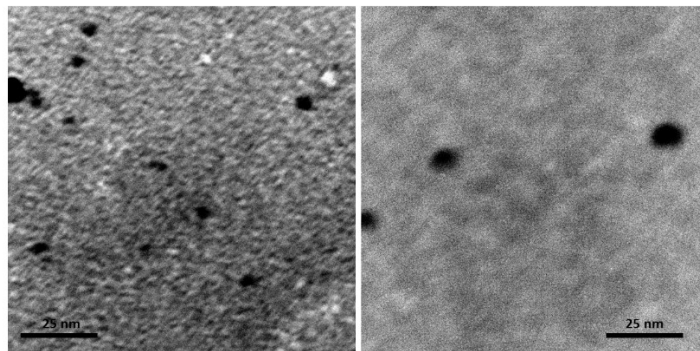


**Fig. S1:** TEM images of 2 nm (left) and 10 nm (right) ZnO nanoparticles.

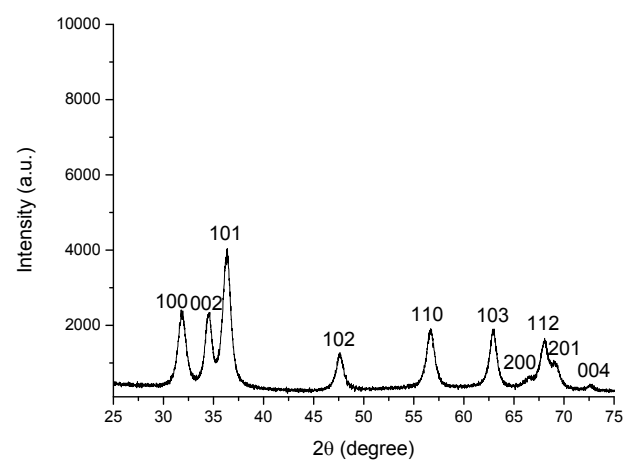


**Fig S2:** XRD spectra of 2 nm TiO<sub>2</sub> nanoparticles.

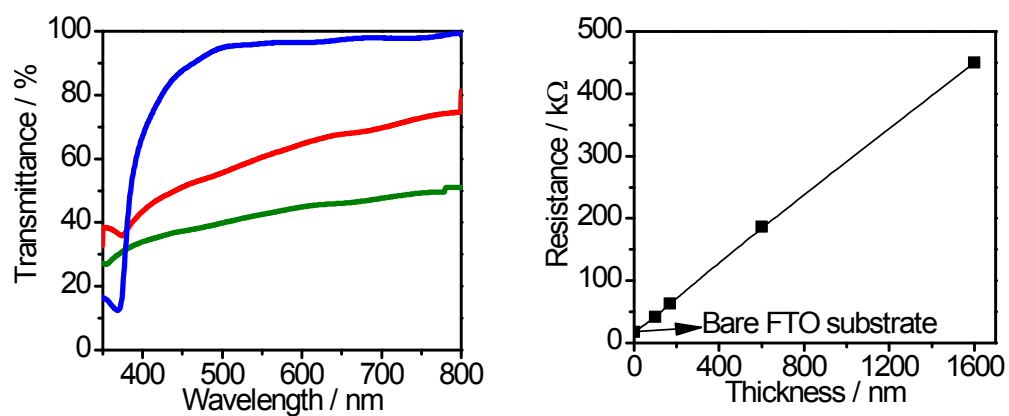


**Fig. S3** Left: Transmittance spectra of the buffer layers with 1600 (green), 600 (red) and 100 (blue) nm thickness. Right: Bulk resistance of the buffer layer vs. its thickness.

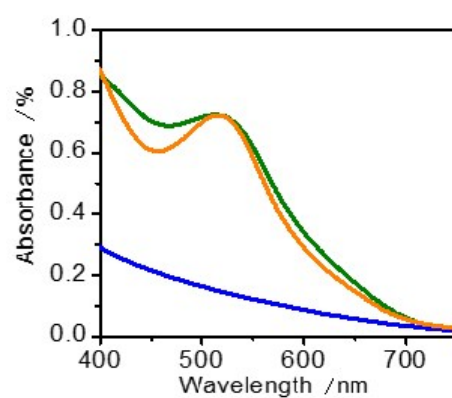


**Fig. S4.** Absorption spectra of pure buffer layer (blue) and sensitized transparent electrode with (green) and without (orange) buffer layer.

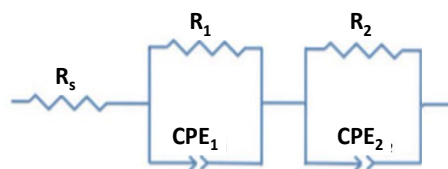


**Fig. S5** The circuit model used for the fitting of the EIS.

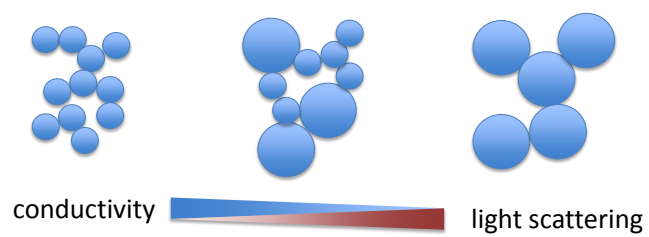


**Fig. S6** A sketch depicting the proposed relationship between the nanoparticle size and the effect on the electron conductivity and the light-scattering features.



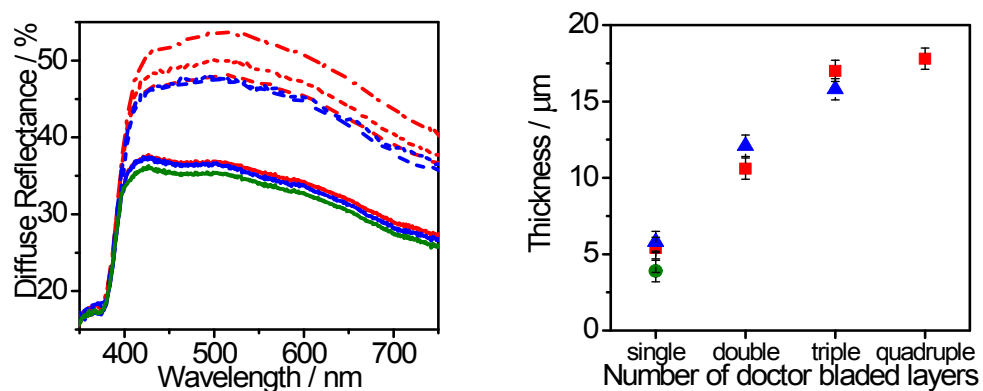


**Fig. S7** Left: Diffuse reflectance spectra of the light-scattering electrodes prepared from the different pastes with different thicknesses, namely single layer (—), double layer (—), triple layer (---), quadruple layer (---). Right: Thickness of the light-scattering electrodes upon increasing the number of doctor-blading steps. The color code refers to electrodes made of pastes with 1:5 (red squares), 1:10 (blue triangles), and 1:20 (green circles) mass ratios.

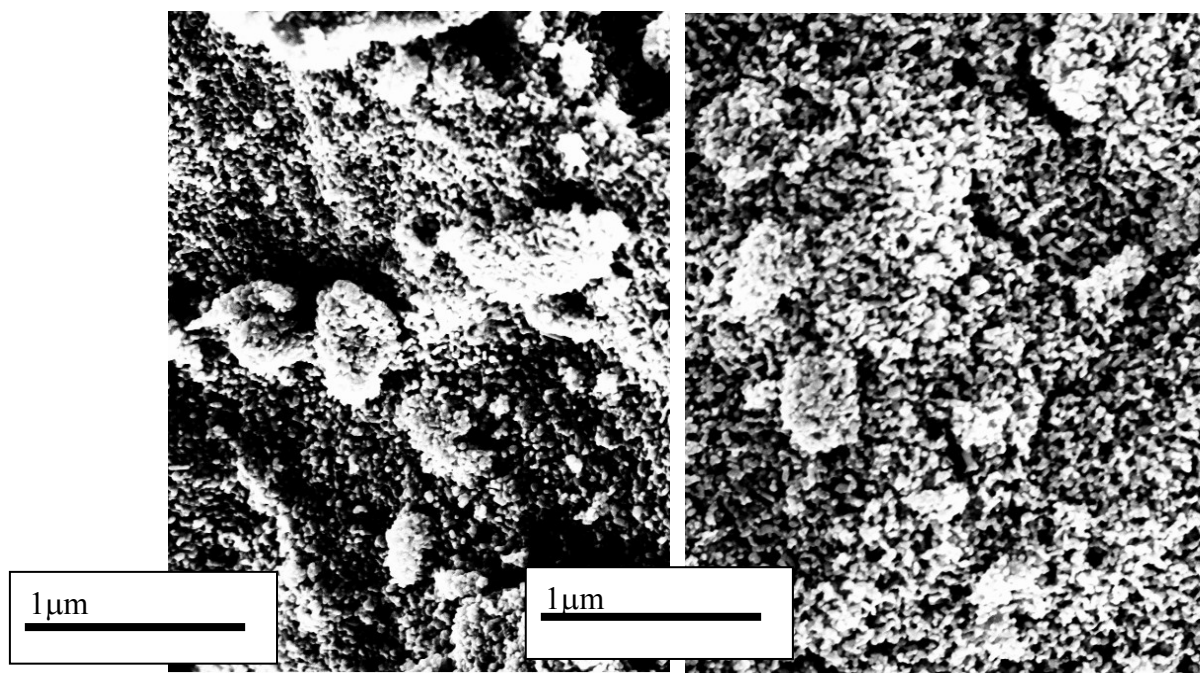


**Fig. S8** SEM pictures of the light-scattering electrodes made of the 1:10 (left) and the 1:20 (right) pastes.

**Table S1** Photovoltaic performance and EIS data of devices with an electrode architecture that consists of a transparent electrode with and without a buffer layer.

Buffer layer	$V_{oc}$ [V]	$J_{sc}$ [mA/cm <sup>2</sup> ]	$J_{scint}$ [mA/cm <sup>2</sup> ]	$FF$ [%]	$\eta$ [%]	$R_w$ [ $\Omega$ ]	$R_k$ [ $\Omega$ ]	$C$ [ $\mu$ F]	$\eta_{coll}$ [%]
None	0.71	4.70	4.44	56	1.86	204	288	11.01	29.17
100 nm	0.73	6.45	6.20	64	3.01	142	392	14.60	63.76

**Table S2** Photovoltaic performance of devices prepared with light-scattering electrodes featuring different compositions and thicknesses.

Electrode composition <sup>[a]</sup>	Electrode thickness [ $\mu$ m]	$V_{oc}$ [V]	$J_{sc}$ [mA/cm <sup>2</sup> ]	$FF$ [%]	$\eta$ [%]
1:5 sg	5.40	0.68	4.20	54	1.54
1:5 db	10.60	0.65	5.78	54	2.02
1:5 tp	14.50	0.63	7.01	57	2.52
1:5 qd	17.80	0.64	8.36	62	3.33
1:10 sg	5.40	0.65	4.36	55	1.56
1:10 db	12.10	0.65	6.40	58	2.41
1:10 tp	15.80	0.64	7.72	60	2.88
1:20 sg	3.90	0.61	2.52	57	0.88

[a] The ratio describes the mixing mass ratio of 10 to 20 nm nanoparticles, while sg, db, tp and qd refers to the number of doctor-blading steps as 1, 2, 3, and 4, respectively.

**Table S3** EIS data of devices prepared with light-scattering electrodes featuring different compositions.

Electrode composition <sup>[a]</sup>	$R_w$ [ $\Omega$ ]	$R_k$ [ $\Omega$ ]	$C$ [ $\mu$ F]	$\tau_{eff}$ [ms]	$L_{eff}$ [ $\mu$ m]	$\eta_{coll}$ [%]
1:5	84.80	180	51.10	30	7.87	52.89
1:10	91.60	180	46.50	30	7.71	49.11
1:20	135.0	263	28.20	24	5.44	48.67

[a] The ratio describes the mixing mass ratio of 10 to 20 nm particles in the paste.

**Table S4** Photovoltaic performance of device with an all-in-one electrode architecture upon different soaking times in N719 solution.

Immersion time [h]	$V_{oc}$ [V]	$J_{sc}$ [mA/cm <sup>2</sup> ]	$FF$ [%]	$\eta$ [%]
1.5	0.69	9.51	63	4.13
3	0.67	11.79	64	5.06
6	0.62	9.90	62	3.81

## References

1. R. Marczak, F. Werner, R. Ahmad, V. Lobaz, D. M. Guldi and W. Peukert, *Langmuir*, 2011, **27**, 3920-3929.
2. For UV/Vis vs. TEM characterization (Figure 4): D. Segets, J. Gradl, R. K. Taylor, V. Vassilev and W. Peukert, *ACS Nano*, 2009, **3**, 1703-1710.
3. D. Segets, R. Marczak, S. Schäfer, C. Paula, J.-F. Gnichwitz, A. Hirsch and W. Peukert, *ACS Nano*, 2011, **5**, 4658-4669.
4. L. Spanhel and M. A. Anderson, *J. Am. Chem. Soc.*, 1991, **113**, 2826-2833.
5. R. Marczak, D. Segets, M. Voigt and W. Peukert, *Adv. Powder Technol.*, 2010, **21**, 41-49.
6. O. I. Micic, C. J. Curtis, K. M. Jones, J. R. Sprague and A. J. Nozik, *J. Phys. Chem.*, 1994, **98**, 4966-4969.
7. N. S. Pesika, K. J. Stebe and P. C. Searson, *J. Phys. Chem. B*, 2003, **107**, 10412-10415.
8. R. Viswanatha and D. D. Sarma, *Chem. – A Eur. J.*, 2006, **12**, 180-186.
9. L. Bergstrom, A. Meurk, H. Arwin and D. J. Rowcliffe, *J. Am. Chem. Soc.*, 1996, **79**, 339-348.
10. R. Viswanatha, S. Sapra, B. Satpati, P. V. Satyam, B. N. Dev and D. D. Sarma, *J. Mater. Chem.*, 2004, **14**, 661-668.
11. For UV/Vis vs. TEM (Figure 2): D. Segets, L. Martinez Tomalino, J. Gradl and W. Peukert, *J. Phys. Chem. C*, 2009, **113**, 11995-12001
12. For UV/Vis vs. SAXS vs. analytical ultracentrifugation (AUC) (Figure 4): T. Schindler, J. Walter, W. Peukert, D. Segets, and T. Unruh, *J. Phys. Chem. B*, 2015, **119**, 15370-15380